

Corrosion Resistance Properties of Expired Granisetron Drug as an Inhibitor for Mild Steel in 1 M HCl

S. Musthafa Kani¹, M. Anwar Sathiq^{1*} and S. S. Syed Abuthahir¹

¹PG and Research Department of Chemistry, Jamal Mohamed College (Autonomous),
Affiliated to Bharathidasan University, Tiruchirappalli- 620 020, India

*Corresponding author: E-mail: anwarchemsathiq@gmail.com

Received 01/05/2023; accepted 01/10/2023

<https://doi.org/10.4152/pea.2025430104>

Abstract

1-Methyl-N-((1R,3r,5S)-9-methyl-9-azabicyclo[3.3.1]nonan-3-yl)-1H-indazole-3-carboxamide (C₁₈H₂₄N₄O: EGS) is used to prevent nausea and vomiting caused by cancer chemotherapy and radiation therapy. It works by blocking serotonin, a natural substance in the body that causes nausea and vomiting. After expiry, it can be used as additive or CI. IE% of EGS on MS corrosion in a 1 M HCl medium was herein evaluated by WL method. WL measurements showed that corrosion IE% increased with higher Ct of EGS, and its maximum value was obtained with 0.001 M. T affects CR. At high T, corrosion IE% decreased, and CR increased. The mechanistic aspects of corrosion resistance have been studied by PDP and EIS. PDP technique revealed that EGS system functioned as an inhibitor of cathodic type, controlling cathodic reactions. It was noted that, with EGS, i_{corr} decreased and LPR increased. EIS studies revealed that a protective film (blanket effect) was formed on the MS surface, since, with EGS, R_{ct} increased and C_{dl} decreased. MS surface morphology with EGS was analyzed by SEM. The constituent elements on the MS surface were characterized by EDX. R_a of MS polished, without and with EGS, was characterized by AFM. The results clearly showed that EGS has high IE% for MS corrosion in HCl.

Keywords: acidic solutions; AFM; CI; EDX, EIS; EGS; IE(%); MS; PDP; SEM.

Introduction*

Corrosion is the destruction of metals due to chemical interaction or electrochemical reaction with their environment. MS is an alloy that can be used in industries for functional and aesthetic purposes. It is largely employed in manufacturing applications such as machinery, due to its work ability without defects, and economic feasibility [1, 2]. Acidic solutions are generally used for the removal of rust and scale in industrial processes. HCl is widely used in steel and ferrous alloys pickling,

* The abbreviations and symbols definition lists are in pages 49-50.

cleaning and descaling. CI are often used in these processes to control metal dissolution [3-5]. The role of an inhibitor is to form a barrier against acid attack. The protective action is often associated with chemical or physical adsorption involving a variation in the charge of the adsorbed substance and its transfer from one phase to the other. Most organic inhibitors for steel corrosion in different aggressive media are organic compounds containing N, S, O and P atoms, or N-hetero cyclic compounds with polar groups. These groups of atoms or bonds facilitate electronic interactions between organic CI and metal surfaces, thereby aiding their adsorption onto steel. In the past few years, the quest for eco-friendly compounds as CI has shifted the research focus onto exploring the potential application of expired drugs [6-15]. Recently, many expired drugs have been reported to be very effective CI for MS protection against acidic media, to promote eco-friendly environments [16-19].

Most drugs work effectively in the corrosive blood environment of our body. This led to the motivation of the present study to find out the effect of expired EGS on MS protection in an acidic solution. Herein, MS corrosion resistance properties due to EGS were investigated in HCl solutions by WL and electrochemical methods. MS surface morphologies were assessed by SEM, EDX and AFM techniques. EGS excellence as CI or additive is based on its environmentally friendliness, since its molecules have N and O as active center atoms.

Experimental techniques

Materials

MS specimens were made from the same sheet of the following composition: C - 0.1%, S - 0.026%, P - 0.06%, Mn - 0.4% and the balance Fe. MS specimens with dimensions $1.0 \times 4.0 \times 0.2$ cm were polished to mirror finish, degreased with trichloroethylene, and used for WL and surface examination studies.

MS specimen encapsulated in Teflon with an exposed cross section of 1cm^2 was used as working electrode in PDP studies. The electrode surface was polished to mirror finish and degreased with trichloroethylene. 1 M HCl was prepared by diluting HCl analytical grade with double distilled water. MS cylindrical rods of the same composition, embedded in PTFE, with an exposed area of 1 cm^2 , were used for PDP and EIS measurements. The electrode was polished using a sequence of emery papers of different grades, and then degreased with acetone.

All chemicals used in this work were of analytical grade, and the solutions were prepared using distilled water. Stock solutions from the examined EGS were prepared by liquefying the suitable weight of pure solid drug in double distilled water. The test solutions were prepared using a 1 M HCl solution with various Ct of EGS. The blank solution was used for comparisons. All tests were done at room T, in magnetically stirred solutions.

Inhibitor characteristics

The inhibitor compound was purchased as expired EGS drug from a pharmaceutical store. EGS name and molecular structure is given in Fig. 1.

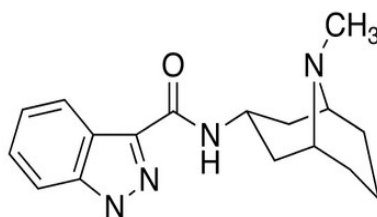


Figure 1: 1-Methyl-N-((1R,3r, 5S)-9-methyl-9-azabicyclo[3.3.1]nonan-3-yl)-1H-indazole-3-carboxamide.

EGS, with molecular weight of 312.4, is a serotonin 5-HT₃ receptor antagonist used as an antiemetic to treat nausea and vomiting, due to chemotherapy and radiotherapy, which is soluble in water [20]. Its main effect is to reduce the *vagus* nerve activity, which is a nerve that activates the vomiting center in *medulla oblongata*. It does not significantly mitigate vomiting, due to motion sickness. This drug does not have any effect on dopamine receptors or muscarinic receptors.

Inhibitor preparation

Double distilled water was used wherever necessary in the solutions preparation. Analytical grade HCl was taken as such and diluted to the required Ct. The required Ct of EGS stock solution was prepared by dissolving it in a minimum amount of ethanol, and making up to the desired volume with double distilled water. Then, the required volume from EGS stock solution was added to the HCl solution, for obtaining the desired Ct. For all the studies, the same volume of ethanol was used to dissolve EGS.

WL measurements

Weight of the three polished MS specimens was measured before and after immersion in various test solutions of 1 M HCl with different Ct of EGS, for 2 h. IE(%) were calculated from eq. (1) [21, 22].

$$IE = \frac{CR_1 - CR_2}{CR_1} \times 100 \% \quad (1)$$

where CR₁ and CR₂ are CR without and with EGS, respectively. CR, in mmd, was calculating using the following formula:

$$CR \text{ (mpy)} = 5.34 \times W / a \times d \times t \quad (2)$$

where W is WL in gram, a is the specimen area in cm², d is thickness (7.8 cm) and t is IT in h.

Electrochemical study

In the present work, CI of MS immersed in various test solutions was measured by PDP study. EIS measurements were performed in a CHI- electrochemical work station with impedance model 660A.

Polarization study

Polarization studies were carried out in a three-electrode cell assembly (Fig. 2). SCE, Pt and MS were reference, counter and working electrodes, respectively. From the polarization study, corrosion parameters such as E_{corr} , I_{corr} , β_a , β_c and LPR values were measured [23, 24].

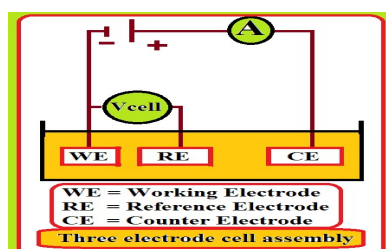


Figure 2: Three electrode cell assembly.

AC impedance spectra

The same instrument and set-up used for polarization study was employed to record AC impedance spectra. A time interval of 5 to 10 min was given for the system to attain OPC steady state. The real (Z') and imaginary ($-Z''$) parts of the cell impedance were measured in ohms, at various frequencies. AC impedance spectra were recorded with initial potential (V) of 0, high ($1-10^5$ Hz) and low (1 Hz) frequencies, amplitude (V) of 0.005 and quiet time (s) of 2. From Nyquist plot, R_{ct} and C_{dl} values were calculated [25, 26].

Surface examinations

MS specimens were immersed in HCl without and with EGS, at various Ct, for 2 h. Then, the samples were taken out and dried. The nature of the film formed on the MS surface was analyzed by SEM, EDX and AFM surface analytical techniques.

SEM analysis

MS specimens immersed in various test solutions for 2 h were taken out, rinsed with double distilled water, dried and subjected to surface examination [27]. Surface morphology measurements of the MS surface were carried out by SEM (JEOL MODEL JSM 6390).

EDX analysis

The elements present on the MS surface immersed in HCl, for 2 h, with and without EGS, were examined by EDX. Then, they were removed, quickly rinsed and dried. The analysis was performed on Quantex 200 with X Flash-6130 EDX.

AFM analysis

The MS specimens immersed, for one day, in various test solutions, were taken out, rinsed with double distilled water, dried and subjected to surface examination [28].

MS surface morphology measurements were carried out by AFM, using SPM Veeco di Innova connected with the software version V7.00, at the scan rate of 0.7 Hz.

Results and discussion

WL measurements

CR and corrosion IE(%) were determined by WL method, before and after MS immersion in 1 M HCl. Corrosion parameters obtained by WL method, such as CR of MS immersed in 1 M HCl without and with expired EGS drugs, and their IE(%), are given in Table 1. It is seen that 0.001 M EGS gave 93.88 IE(%). With higher Ct of EGS, corrosion protection properties increased. This was due to an increase in the SC of MS by EGS, at higher Ct, which hindered its dissolution. The interface between hetero atoms in EGS and ions from the MS surface was due to higher IE(%). The occurrence of active constituents in EGS may be accountable for CI of MS, due to its anti-corrosive properties. The same hypothesis has been reported by [29-33].

Table 1: CR, IE(%) and SC of MS immersed in 1 M HCl with various Ct of EGS, obtained by WL method, at 303 K.

1 M HCl				
S. No	Ct of EGS (M)	CR (mpy)	IE(%)	SC (θ)
1	blank	0.8386	-	-
2	0.0000001	0.2995	64.28	0.6428
3	0.000001	0.2396	71.45	0.7145
4	0.00001	0.1797	78.57	0.7857
5	0.0001	0.1112	86.73	0.8673
6	0.001	0.0513	93.88	0.9388

Effect of T

The effect of T on MS corrosion in HCl with and without EGS is shown in Table 2. It can be seen that WL increased with higher T, without and with inhibitor. At high T, MS dissolution increased, and underwent severe corrosion. In electrochemical studies, T influence on the adsorption mechanism of EGS molecules onto the MS surface of demonstrates its main role. In fact, corrosion IE(%) of EGS and CR of MS were investigated for EGS inhibitor system, from 0.0000001 to 0.001 M, with T from 303 to 333 K [34]. IE(%) and CR values are given in Table 2.

Table 2: Values for CR of MS, and IE(%) and SC of 0.001 M EGS, for various T, in 1 M HCl.

1 M HCl				
S. No	T (K)	CR (mpy)	IE(%)	SC (θ)
1	303	0.0513	93.88	0.938
2	308	0.0855	89.8	0.898
3	313	0.1283	84.7	0.847
4	318	0.2225	73.46	0.734
5	323	0.3508	58.16	0.581
6	328	0.4535	45.92	0.459
7	333	0.5648	32.64	0.326

IE(%) decreased from 93.88 to 32.64%, and CR increased from 0.0513 to 0.5648 (mpy), with a rise in T from 303 to 333 K, in 1 M HCl, at the maximum Ct (0.001 M) of EGS. T effect on MS dissolution and EGS molecules partial desorption from the metal surface increased with the inhibitor higher Ct [35].

PDP studies

PDP technique has been applied to observe the development of a defensive layer on the MS surface [36]. When a protective film was developed on the MS surface, LPR values increased and i_{corr} decreased. PDP arcs of MS submerged in 1 M HCl without and with EGS are shown in Fig. 3.

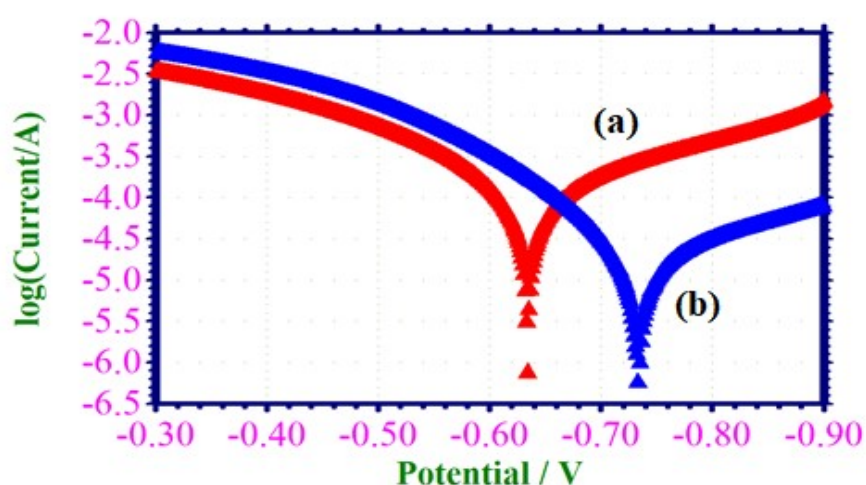


Figure 3: PDP arcs for MS corrosion in 1 M HCl: (a) without EGS; (b) with 0.001 M EGS.

Corrosion parameters, namely, E_{corr} , β_c , β_a , LPR and I_{corr} , are given in Table 3.

Table 3: PDP parameters for MS corrosion in 1 M HCl without and with EGS.

Ct of EGS (M)	E_{corr} mV/SCE	Tafel slopes		I_{corr} A/cm ²	LPR Ω/cm ²
		β_a mV/dec	β_c mV/dec		
blank	- 632	0.152	0.208	1.2730×10^{-4}	291
0.001	- 732	0.104	0.235	2.2010×10^{-5}	1502

Fig. 3a shows that, for MS immersed in 1 M HCl, E_{corr} was -632 mV vs. SCE. LPR value was 291 ohm/cm². Value of i_{corr} was 1.2730×10^{-4} A/cm².

E_{corr} shifted to the cathodic side (-732 mV vs. SCE) when 0.001 M EGS was added to 1 M HCl, due to the formation of a defensive layer on the MS surface (Fig. 3b). This film controlled the cathodic reaction of MS dissolution, by forming a Fe²⁺-EGS complex on the cathodic sites of the metal surface [37-41]. EGS acts as cathodic type inhibitor, because, E_{corr} shift went towards a more negative side

than that of the blank. Increase in LPR and decrease in I_{corr} values indicate the strong corrosion resistant nature of the inhibitor system.

Analysis of AC impedance spectra

EIS have been used to validate the development of a defensive layer on the MS surface [42-44]. If a defensive layer is formed on the MS surface, R_{ct} increases, C_{dl} decreases and impedance $\log(z/\text{ohm})$ increases. AC impedance spectra of MS immersed in 1 M HCl, without and with EGS, are shown in Fig. 4 (Nyquist plots), and the values are given in Table 4.

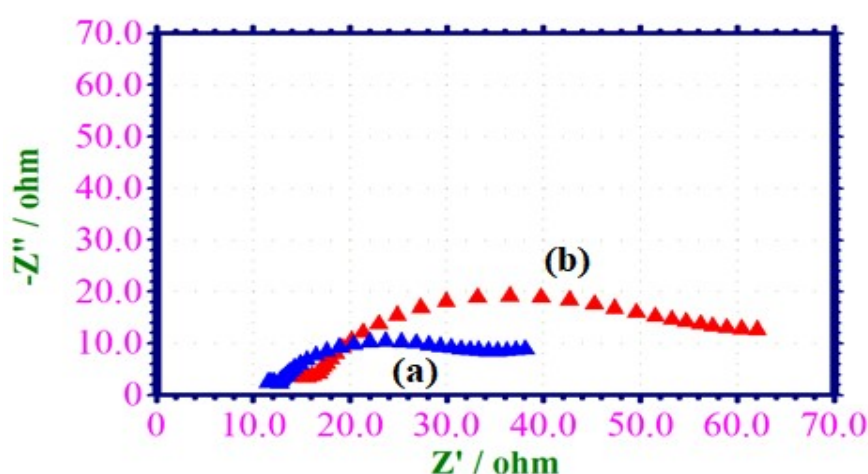


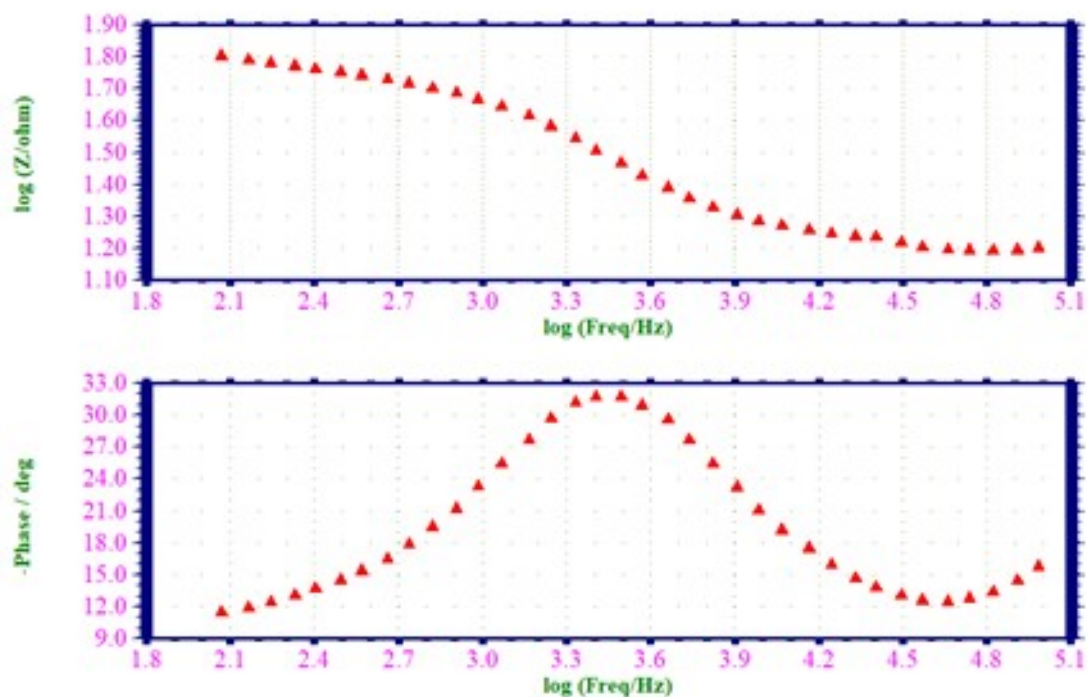
Figure 4: AC impedance spectra of MS immersed in: (a) 1 M HCl without EGS; and (b) 1 M HCl with 0.001 M EGS (Nyquist plots).

Table 4: EIS parameters from Nyquist plots for corrosion of MS immersed in 1 M HCl without and with EGS.

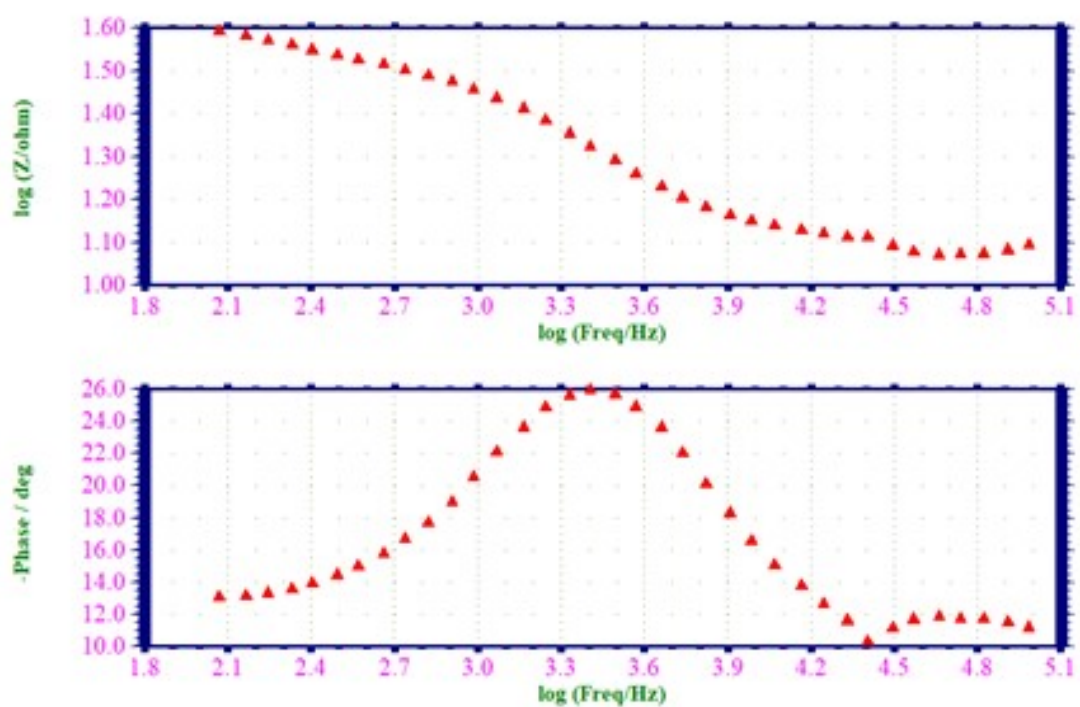
Ct of EGS (M)	Nyquist plot		Impedance log (z/ohm)	Phase angle (°)
	R_t Ω/cm^2	C_{dl} F/cm^2		
blank	23.69	42.3779×10^{-6}	0.502	25.9
0.001	46.76	76.6604×10^{-6}	0.604	31.9

When MS was immersed in 1 M HCl, LPR value was $23.62 \text{ ohm}/\text{cm}^2$, and C_{dl} value was $42.3779 \times 10^{-6} \text{ F}/\text{cm}^2$. LPR value increased from 23.62 to $46.76 \text{ ohm}/\text{cm}^2$, when 0.001 M EGS was added to 1 M HCl. C_{dl} value also decreased from 42.3779×10^{-6} to $76.6604 \times 10^{-6} \text{ F}/\text{cm}^2$. Impedance value [$\log(z/\text{ohm})$] increased from 0.502 to 0.604. Furthermore, the inhibitor system phase angle increased from 25.9 to 31.9° , when compared to the blank system [45-47]. This suggests that a defensive layer was formed on the MS surface.

Fig. 5 shows Bode plots.



(a)



(b)

Figure 5: AC impedance spectra of MS immersed in 1 M HCl (Bode plot); (a) blank; and (b) with 0.001 M EGS (Bode Plot).

MS surface analysis by SEM

SEM pictures of the MS surface are examined without and with EGS [48, 49], to understand the nature of the coating developed in the inhibitor absence and presence, and the extent of metallic corrosion [50]. SEM images of MS immersed in 1 M HCl, for 2 h, without and with EGS, are shown in Figs. 6 (a-c) respectively.

Images of polished MS are shown (control) in Fig. 6a, which depict its smooth surface. The MS surface was corroded due to its dissolution in 1 M HCl (blank) (Fig. 6b), and it is rough. CR of the MS surface immersed in 1 M HCl with 0.001 M EGS (Fig. 6c) was suppressed, as it can be seen from the decrease in corroded areas. MS is almost free from corrosion, due to the formation of an insoluble complex on its surface. MS surface smoothness is almost equal to the polished one [51], as it was covered by a thin layer of EGS, which controlled its dissolution in 1 M HCl.

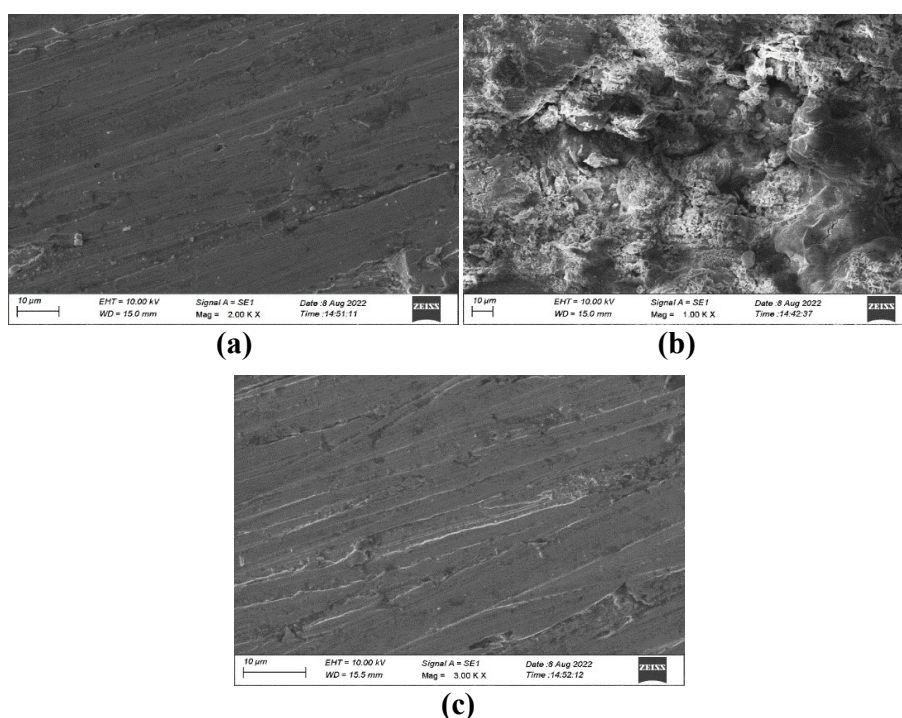


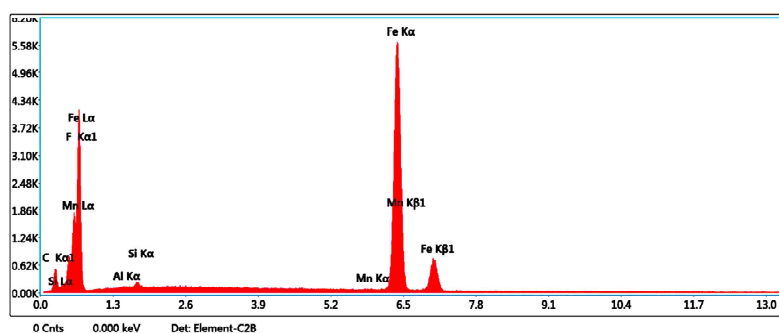
Figure 6: SEM image of MS coupon- (a) polished; (b) after immersion in 1 M HCl (blank); (c) after immersion in 1 M HCl with 0.001 M EGS.

Surface characterization of MS by EDX

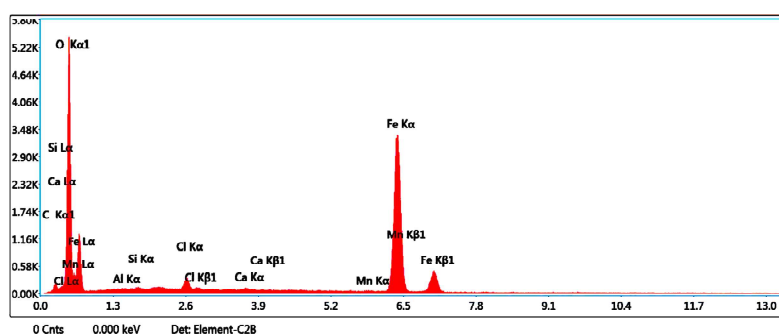
EDX examinations of the MS surface were performed in the absence and presence of EGS system. EDX spectra have been used to determine the elements present on the MS surface before and after exposure to EGS [52-54].

EDX spectrum of MS (Fig. 7a) shows the characteristic peaks of some of the elements constituting the MS sample. EDX spectrum of MS immersed in 1 M HCl (Fig.7b) shows the dissolution in MS constituting elements. Moreover, Cl⁻ presence

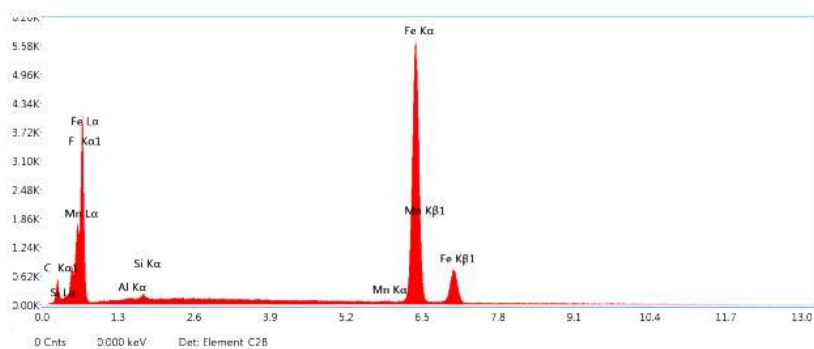
caused MS damages by 1 M HCl. EDX spectrum of MS immersed in 1 M HCl and 0.001 M EGS (Fig. 7c) shows an additional line characteristic of Cl signals reduced intensity and of MS surface constituting elements increased strength signal. Fe signal appearance and O signal enhancement are due to EGS presence. These data show that the CS surface was covered with Fe, S, C, P, Ni, N and O atoms.



(a)



(b)



(c)

Figure 7: EDX spectra of MS specimen- (a) control; (b) immersed in 1 M HCl (blank); (c) immersed in 1 M HCl with 0.001 M EGS.

MS surface analysis by AFM

Figs. 8a-c show AFM morphologies and cross-sectional profiles for the MS surface: polished (control sample), in 1 M HCl (blank sample); and in 1 M HCl with 0.001 M EGS.

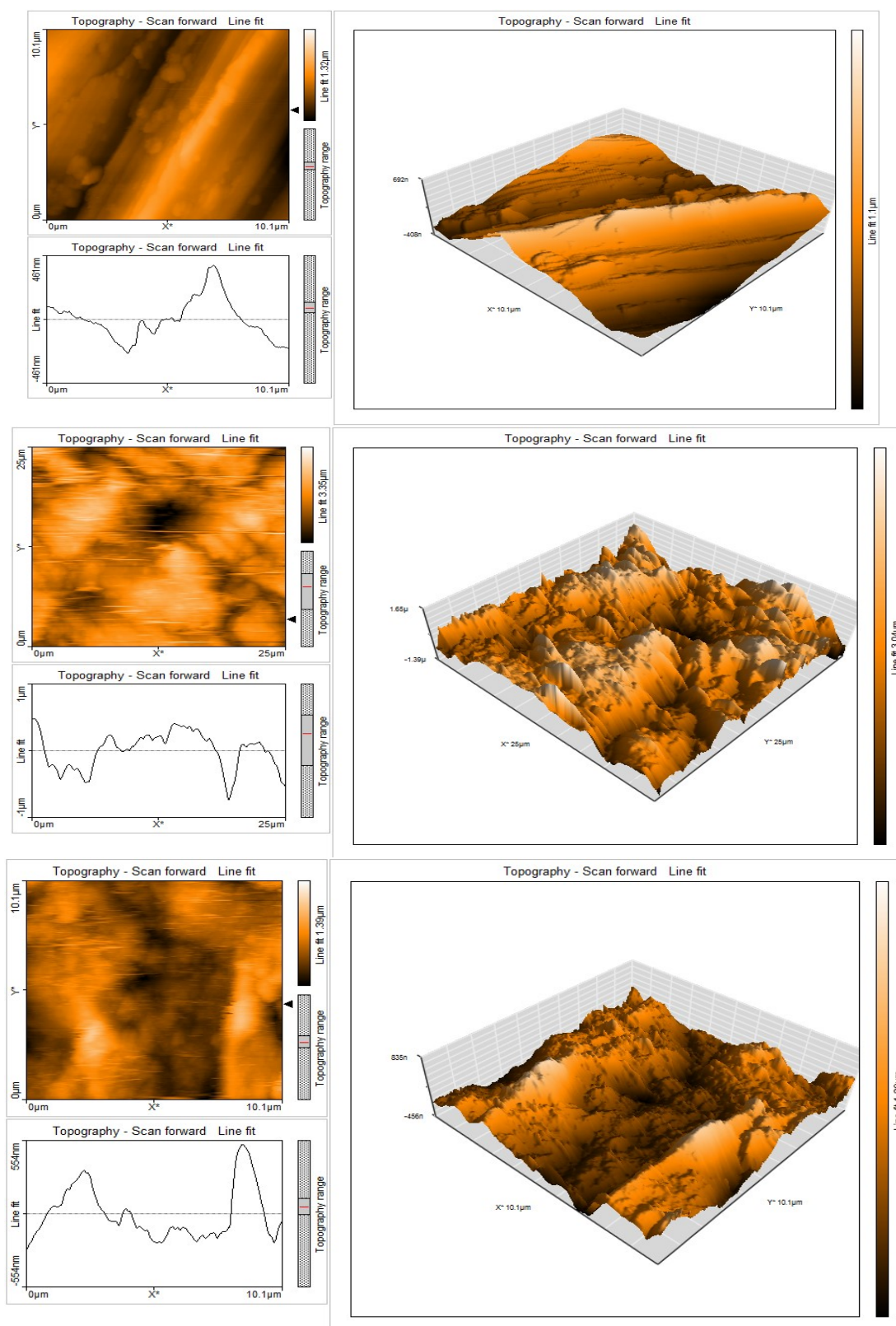


Figure 8: AFM cross sectional image of MS surfaces- **(a)** polished (control); **(b)** after immersion in 1 M HCl (blank); **(c)** after immersion in 1 M HCl with 0.001 M EGS.

Roughness in any surface is easily investigated by AFM studies. AFM provides direct insight into the changes in the surface morphology that take place at several hundred nanometers [55].

Topographical changes took place in the MS surface, i.e., corrosion and formation of a protective layer on its surface, without and with EGS, respectively. Herein, EGS effect on the MS surface corrosion in HCl was examined by AFM. This characterization contains three dimensional (3D images).

AFM images analyses were performed to obtain: the area and line surface roughness - S_a and R_a (average deviation of all points roughness profile from a mean line over the evaluation length); S_q and R_q (root-mean-square surface roughness- the average of the measured height deviations taken within the evaluation length and measured from the mean line); S_y and R_y (largest single peak-to-valley height in five adjoining sampling heights); and S_p and R_p (maximum profile peak height), which indicates the point along the sampling length at which the curve is highest.

AFM parameters for area and line surface roughness are given in Tables 5 and 6, respectively.

Table 5: AFM data for MS immersed in HCl without and with EGS (area roughness).

MS surface samples	S_a nm	S_q nm	S_y nm	S_p nm
Polished	136.47	168.68	892.96	476.88
In 1 M HCl	379.59	476.21	3295.4	1530.6
In 1 M HCl+ 0.001 M EGS	155.57	187.28	1149.6	639.8

Table 6: AFM data for MS immersed in HCl without and with EGS (line roughness).

MS surface samples	R_a nm	R_q nm	R_y nm	R_p nm
Polished	119.44	161.1	684.87	406.66
In 1 M HCl	344.72	393.18	1359.9	726.51
In 1 M HCl+ 0.001 M EGS	181.52	199.83	675.66	365.55

S_a and R_a values for CS in HCl (blank) are the highest. With 0.001 M EGS, this value decreased, but is higher than that of the polished MS surface, because the inhibitor formed a layer that covered the MS surface. This film was found to be smooth. The same happened with S_q , R_q , S_y , R_y and S_p and R_p [56, 57].

Conclusions

In the present study, EGS inhibition of MS corrosion in 1 M HCl was tested. With higher Ct of EGS, an increase in its IE(%) and a decrease in CR of MS in 1 M HCl medium were observed. 0.001 M EGS obtained maximum IE(%) of 93.88%. PDP studies revealed that EGS performed as a cathodic type of inhibitor. According to EIS, there was an increase in LPR and a decrease in C_{dl} . This behavior was due to the formation of a dense protective layer on the MS/HCl surface, which was characterized by SEM. Furthermore, EDX showed MS smoother surface with EGS

than without it. R_a value of MS was lower than that of the blank, and higher than that of the polished sample, which was confirmed by AFM. EGS acted as an efficient inhibitor of MS corrosion in a 1 M HCl medium. The outcome of the study may find application in the pickling industry.

Acknowledgements

The authors are thankful to the Principal and College Management Committee Members of Jamal Mohamed College (Autonomous), for providing necessary facilities, and to DBT and DST-FIST, for providing instrumental facilities to carry out research work.

Authors' contributions

S. Musthafa Kani: contributed to writing of the original draft, validation, investigation, supervision and methodology. **M. Anwar Sathiq:** contributed to review and editing. **S. S. Syed Abuthahir:** involved in the characterization analysis of the study.

Abbreviations

AC: alternating current
AFM: atomic force microscopy
 C_{dl} : double layer capacitance
CI: corrosion inhibitor/inhibition
CR: corrosion rate
Ct: concentration
 E_{corr} : corrosion potential
EDX: energy-dispersive X-ray spectroscopy
EGS: Granisetron ($C_{18}H_{24}N_4O$)
EIS: electrochemical impedance spectroscopy
HCl: hydrochloric acid
 I_{corr} : corrosion current
IE%: inhibition efficiency
IT: immersion time
LPR: linear polarization resistance
MS: mild steel
OCP: open circuit potential
PDP: potentiodynamic polarization
PTFE: polytetrafluoroethylene
 R_a : average surface roughness
 R^2 : regression coefficient
 R_{ct} : charge transfer resistance
SC: surface coverage (θ)
SCE: saturated calomel electrode
SEM: scanning electron microscopy
T: temperature
WL: weight loss

Symbols definition

β_a : anodic Tafel slope

β_c : cathodic Tafel slope

References

1. Adewuyi A, Gopfert A, Wolff T. Succinyl amide Gemini surfactant from *Adenopusbreviflorus* seed oil: a potential corrosion inhibitor of mild steel in acidic medium. *Ind Crops Prod.* 2014;52:439-449. <https://doi.org/10.1016/j.indcrop.2013.10.045>
2. Anupama KK, Ramya K, Joseph A. Electrochemical measurements and theoretical calculations on the inhibitive interaction of *Plectranthusamboinicus* leaf extract with mild steel in hydrochloric acid. *Measurement.* 2017;95:297-305. <https://doi.org/10.1016/j.measurement.2016.10.030>
3. Popova A, Sokolova E, Raicheva S et al. AC and DC study of the temperature effect on mild steel corrosion in acid media in the presence of benzimidazole derivatives. *Corros Sci.* 2003;(45)1:33-58. [http://dx.doi.org/10.1016/S0010-938X\(02\)00072-0](http://dx.doi.org/10.1016/S0010-938X(02)00072-0)
4. Noor EA. The inhibition of mild steel corrosion in phosphoric acid solutions by some N-heterocyclic compounds in the salt form. *Corros Sci.* 2005;(47)1:33-35. <https://doi.org/10.1016/j.corsci.2004.05.026>
5. Bouklah M, Hammoutim B, Benkaddour M et al. Thiophene derivatives as effective inhibitors for the corrosion of steel in 0.5 M H₂SO₄. *J Appl Electrochem.* 2005;35:1095-1101. <https://doi.org/10.1016/j.porgcoat.2003.09.014>
6. Ahamad I, Quraishi MA. Mebendazole: New and efficient corrosion inhibitor for mild steel in acid medium. *Corros Sci.* 2010;52:651-656. <https://doi.org/10.1016/j.corsci.2009.10.012>
7. Fouda AS, Al-Sarawy AA, Ahmed FSH et al. Some new triazole derivatives as inhibitors for mild steel corrosion in acidic medium. *J Appl Electrochem.* 2008;38:289-295. <https://doi.org/10.1007/s10800-007-9437-7>
8. Geethamani P, Kasthuri PK. Corrosion inhibition of mild steel in sulphuric acid medium by Ambroxol drug. *J Appl Chem Sci Int.* 2015;3:151-157. <https://doi.org/10.1080/23312009.2015.10915588>
9. Hosseini M, Mertens SFL, Arshadi MR. Synergism and antagonism in mild steel corrosion inhibition by sodium dodecylbenzenesulphonate and hexamethylenetetramine. *Corros Sci.* 2003;45:1473-1489. [https://doi.org/10.1016/S0010-938X\(02\)00246-9](https://doi.org/10.1016/S0010-938X(02)00246-9)
10. Khan S, Quraishi MA. Synergistic effect of potassium iodide on inhibitive performance of thiadiazoles during corrosion of mild steel in 20% sulfuric acid. *Arab J Sci Eng.* 2010;35:71-82.
11. Prabhu RA, Shanbhag AV, Venkatesha TV. Influence of tramadol[2-[(dimethylamino) methyl]-1-(3-methoxyphenyl) cyclohexanol hydrate] on corrosion inhibition of mild steel in acidic media. *J Electroanal Chem.* 2007;37:491-497.

12. Quraishi MA, Rawat J. Corrosion inhibition of mild steel in acid solutions by tetramethyl-dithiooctaazacyclotetradeca hexaene (MTAT). *Anti-Corros Meth Mat*. 2000;47:288-293. <https://doi.org/10.1108/00035590010351549>
13. Quraishi MA, Sardar R, Jamal D. Corrosion inhibition of mild steel in hydrochloric acid by some aromatic hydrazides. *Mat Chem Phys*. 2001;71:309-313. [https://doi.org/10.1016/S0254-0584\(01\)00295-4](https://doi.org/10.1016/S0254-0584(01)00295-4)
14. Umoren SA, Ebenso EE. The synergistic effect of polyacrylamide and iodide ions on the corrosion inhibition of mild steel in H₂SO₄. *Mat Chem Phys*. 2007;106:387-393. <https://doi.org/10.1016/j.matchemphys.2007.06.018>
15. Zhao TP, Mu GN. The adsorption and corrosion inhibition of anion surfactants on aluminium surface in hydrochloric acid. *Corros Sci*. 1999;41:1937-1944. [http://dx.doi.org/10.1016/S0010-938X\(99\)00029-3](http://dx.doi.org/10.1016/S0010-938X(99)00029-3)
16. Ahamad I, Khan S, Quraishi M. Primaquine: A pharmaceutically active compound as corrosion inhibitor for mild steel in hydrochloric acid solution. *J Chem Pharmaceut Res*. 2011;3:703-717.
17. Hari KS, Karthikeyan S. Torsemide and Furosemide as green inhibitors for the corrosion of mild steel in hydrochloric acid medium. *Industr Eng Chem Res*. 2013;52:7457-7469. <https://doi.org/10.1021/ie400815w>
18. Singh, AK, Quraishi MA. Effect of cefazolin on the corrosion of mild steel in HCl solution. *Corros Sci*. 2010;52:152-160. <https://doi.org/10.1016/j.corsci.2009.08.050>
19. Singh A, Singh AK, Quraishi MA. Dapsone: A novel corrosion inhibitor for mild steel in acid media. *Open Electrochem J*. 2010;2:435. <http://dx.doi.org/10.2174/1876505X01002010043>
20. FDA Approves Sancuso, the First and Only Patch for Preventing Nausea and Vomiting in Cancer Patients Undergoing Chemotherapy. *PRNewswire*. September 12, 2008.
21. Rajendran S, Agasta M, Devi RB et al. Corrosion inhibition by an aqueous extract of Henna leaves (*Lawsonia Inermis L*). *Zast Mater*. 2009;50:77-84.
22. Sribharathy V, Rajendran Rengan P et al. Corrosion inhibition by an aqueous extract of *Aloevera* (L) Burm F. (*Liliaceae*). *Eur Chem Bull*. 2013;2:471-476.
23. Kavitha N, Manjula P. Corrosion Inhibition of Water Hyacinth Leaves, Zn²⁺ and TSC on mild steel in neutral aqueous medium. *Int J Nano Corros Sci Eng*. 2014;1:31-38.
24. Thangakani JA, Rajendran S, Sathiyabama J et al. Inhibition of corrosion of carbon steel in aqueous solution containing low chloride ion by glycine – Zn²⁺ system. *Int J Nano Corros Sci Eng*. 2014;1:50-62.
25. Gowri S, Sathiyabama J, Rajendran S et al. Tryptophan as corrosion inhibitor for carbon steel in sea water. *J Chem Biol Phys Sci*. 2012;2:2223-2231.
26. Mary ACC, Rajendran S, Al-Hashem H et al. Corrosion resistance of mild steel in simulated produced water in presence of sodium potassium tartrate. *Int J Nano Corros Sci Eng*. 2015;1:42-50.

27. Saxena A, Prasad D, Haldhar R et al. Use of *Saracaashoka* extract as green corrosion inhibitor for mild steel in 0.5 M H₂SO₄. *J Mol Liq.* 2018;258:89-97.
28. Onat TA, Yiğit D, Nazır H et al. Bio corrosion inhibition effect of 2-amino pyrimidine derivatives on SRB. *Int J Corros Scale Inhib.* 2016;(5)3:273-281. <https://doi.org/10.17675/2305-6894-2016-5-3-7>
29. Fabrizio Z, Ibrahim HO . Plant extracts as corrosion inhibitors of mild steel in HCl solutions. *Surf Technol.* 1985;(24)4:391-399. [https://doi.org/10.1016/0376-4583\(85\)90057-3](https://doi.org/10.1016/0376-4583(85)90057-3)
30. Singh A, Quraishi MA. The extract of *Jamun (Syzygium cumini)* seed as green corrosion inhibitor for acid media *Res Chem Intermed.* 2015;41:2901-2914. <https://doi.org/10.1007/s11164-013-1398-3>
31. Begum AS, Nasser AJA, Sheit HMK et al. *Abrusprecatorius* leaf aqueous extract as a corrosion inhibitor on mild steel in 1.0 M HCl solution. *Int J Sci: Basic Appl Res.* 2019;(9)2:438-450.
32. Tuama RJ, Al-Dokheily ME, Khalaf MN. Recycling and evaluation of poly (ethylene terephthalate) waste as effective corrosion inhibitors for C-steel material in acidic media. *Int J Corros Scale Inhib.* 2020;(9)2:427-445. <https://doi.org/10.17675/2305-6894-2020-9-2-3>
33. Jeeva PA, Mali GS, Dinakaran R et al. The influence of Co-Amoxiclav on the corrosion inhibition of mild steel in 1 N hydrochloric acid solution. *Int J Corros Scale Inhib.* 2019(8)1:1-12. <https://doi.org/10.17675/2305-6894-2019-8-1-1>
34. Hashim NZN, Kassim K. Zaki, Alharthi HM et al. XPS and DFT investigations of corrosion inhibition of substituted benzylidene Schiff bases on mild steel in hydrochloric acid. *Appl Surf Sci.* 2019;476:861-877.
35. Shahabi S, Hamidi S, Ghasemi JB et al. Synthesis, experimental, quantum chemical and molecular dynamics study of carbon steel corrosion inhibition effect of two Schiff bases in HCl solution. *J Mol Liq.* 2019;285:626-639.
36. Fernandes CM, Pina VG, Alvarez LX et al. Use of a theoretical prediction method and quantum chemical calculations for the design, synthesis and experimental evaluation of three green corrosion inhibitors for mild steel. *Coll Surf A: Physicochem Eng Asp.* 2020;599:124857.
37. Karthikeyan S, Abuthahir SSS, Begum AS et al. Thermodynamic, Adsorption and Electrochemical Studies of Mild Steel in 0.5 M HCl Solution by using Green Inhibitor. *Indian J Nat Sci.* 2021;(67)12:33696-33711.
38. Benali O, Larabi L, Traisnel M et al. Electrochemical, theoretical and XPS studies of 2-mercapto-1-methylimidazole adsorption on carbon steel in 1 M HClO₄. *Appl Surf Sci.* 2007;(253)14:6130-6139.
39. Amar H, Braisaz T, Villemin D et al. Thiomorpholin-4-ylmethyl-phosphonic acid and morpholin-4-methyl-phosphonic acid as corrosion inhibitors for carbon steel in natural seawater. *Mat Chem Phys.* 2008;(110)1:1-6.
40. Sangeetha M, Rajendran S, Sathiyabama J et al. Corrosion inhibition by an aqueous extract of *Phyllanthus amarus*. *Port Electrochim Acta.* 2011;(29)6:429-444. <https://doi.org/10.4152/pea.201106429>

41. Kumari PP, Rao SA, Shetty P. Corrosion inhibition of mild steel in 2 M HCl by a Schiff base derivative. *Proced Mat Sci.* 2014;5:499-507.
42. Raja AS, Rajendran S. Inhibition of corrosion of carbon steel in well water by arginine-Zn²⁺ system. *J Electrochem Sci Eng.* 2012;(2)2:91-104.
43. Banu VN, Rajendran S, Abuthahir SSS. Corrosion Inhibition by Self-assembling Nano films of Tween 60 on Mild steel surface. *Int J Chem Concep.* 2017;(1)3:161-165.
44. Heakal FET, Fouda AS, Radwan MS. Inhibitive effect of some thiadiazole derivatives on C-steel corrosion in neutral sodium chloride solution. *Mat Chem Physi.* 2011;125(1-2):26-36.
45. Abuthahir SSS, Nasser AJA. Corrosion behavior of Mild Steel in Sodium. *J Adv Appl Sci Res.* 2017;2454:3225.
46. Jisha M, Hukuman NZ, Leena P et al. Electrochemical, computational and adsorption studies of leaf and floral extracts of *Pogostemon quadrifolius* (Benth.) as corrosion inhibitor for mild steel in hydrochloric acid. *J Mater Environ Sci.* 2019;(9)10:840-853.
47. Baby AG, Rajendran S, Johnsirani V et al. Influence of zinc sulphate on the corrosion resistance of L80 alloy immersed in sea water in the absence and presence of sodium potassium tartrate and trisodium citrate. *Int J Corros Scale Inhib.* 2020;(3)9:979-999.
48. Dehghani A, Bahlakeh G, Ramezanzadeh B et al. Potential role of a novel green eco-friendly inhibitor in corrosion inhibition of mild steel in HCl solution: Detailed macro/micro-scale experimental and computational explorations. *Constr Build Mat.* 2020;245:118464.
49. Rajendran S, Srinivasan R, Dorothy R et al. Green solution to corrosion problems-at a glance. *Int J Corros Scale Inhib.* 2019;(3)8:437-479.
50. Abuthahir SSS, Vijaya K, Nasser AJA et al. Corrosion Inhibition of Mild Steel in Sodium Chloride Solution by Nickel Complex of 1-(8-hydroxy quinolin-2yl-methyl) *Thiourea*. *J Adv Res Appl Sci.* 2015;(2)2:221-27.
51. Gopi D, Govindaraju KM, Manimozhi S et al. Inhibitors with biocidal functionalities to mitigate corrosion on mild steel in natural aqueous environment. *J Appl Electrochem.* 2007;37(6):681-689.
52. Amin MA, Abd El-Rehim SS, El-Sherbini et al. The inhibition of low carbon steel corrosion in hydrochloric acid solutions by succinic acid: Part I. Weight loss, polarization, EIS, PZC, EDX and SEM studies. *Electrochim Acta.* 2007;52(11):3588-3600.
53. Gopi D, Manimozhi SGKM, Govindaraju KM et al. Surface and electrochemical characterization of pitting corrosion behaviour of 304 stainless steel in ground water media. *J Appl Electrochem.* 2007;(37)4:439-449.
54. Raja AS, Rajendran S. Inhibition of corrosion of carbon steel in well water by arginine-Zn²⁺ system. *J Electrochem Sci Eng.* 2012;2(2):91-104.
55. Amin MA, Abd El RSS, Abdel-Fatah HT. Electrochemical frequency modulation and inductively coupled plasma atomic emission spectroscopy methods for monitoring corrosion rates and inhibition of low alloy steel corrosion in HCl solutions and a test for validity of the Tafel extrapolation method. *Corros Sci.* 2009;(51)4:882-894.

56. Kıcır N, Tansuğ G, Erbil M *et al.* Investigation of ammonium (2, 4-dimethylphenyl)-dithiocarbamate as a new, effective corrosion inhibitor for mild steel. *Corros Sci.* 2016;105:88-99.
57. Amin MA, Abd El-Rehim SS, El-Sherbini EEF *et al.* The inhibition of low carbon steel corrosion in hydrochloric acid solutions by succinic acid. Part I. Weight loss, polarization, EIS, PZC, EDX and SEM studies. *Electrochim Acta.* 2007;(52)11:3588-3600. <https://doi.org/10.1016/j.electacta.2006.10.019>